Ancient *Austrocedrus* Tree-Ring Chronologies Used to Reconstruct Central Chile Precipitation Variability from A.D. 1200 to 2000

CARLOS LE QUESNE

Instituto de Silvicultura, Universidad Austral de Chile, Valdivia, Chile

DAVID W. STAHLE, MALCOLM K. CLEAVELAND, AND MATTHEW D. THERRELL

Department of Geosciences, University of Arkansas, Fayetteville, Arkansas

JUAN CARLOS ARAVENA

Centro de Estudios Cuaternarios (CEQUA), Universidad de Magallanes, Punta Arenas, Chile

JONATHAN BARICHIVICH

Instituto de Silvicultura, Universidad Austral de Chile, Valdivia, Chile

(Manuscript received 31 May 2005, in final form 20 March 2006)

ABSTRACT

An expanded network of moisture-sensitive tree-ring chronologies has been developed for central Chile from long-lived cypress trees in the Andean Cordillera. A regional ring width chronology of cypress sites has been used to develop well-calibrated and verified estimates of June–December precipitation totals for central Chile extending from A.D. 1200 to 2000. These reconstructions are confirmed in part by historical references to drought in the seventeenth and eighteenth centuries and by nineteenth-century observations on the position of the Río Cipreses glacier. Analyses of the return intervals between droughts in the instrumental and reconstructed precipitation series indicate that the probability of drought has increased dramatically during the late nineteenth and twentieth centuries, consistent with selected long instrumental precipitation records and with the general recession of glaciers in the Andean Cordillera. This increased drought risk has occurred along with the growing demand on surface water resources and may heighten socioeconomic sensitivity to climate variability in central Chile.

1. Introduction

Proxy indicators of effective precipitation in central Chile suggest a secular decline in annual precipitation and/or an increase in temperature over the past 200 yr (Boninsegna 1988; Villalba 1994a; Rivera et al. 2000; Luckman and Villalba 2001). Several long instrumental precipitation records from the region also indicate a significant long-term decline since the midnineteenth century (e.g., Luckman and Villalba 2001). These apparent long-term precipitation changes are occurring simultaneously with the growing agricultural, industrial, and municipal consumption of water in central Chile and may lead to increased socioeconomic sensitivity to climate variability and change. For example, half of the population of Chile lives in the central part of the country (INE 2003) and is highly dependent on water supply from the snow and ice fields of the Andes Cordillera (Masiokas et al. 2006). The droughts of 1968, 1996, 1998, and 1999 caused severe restrictions of water supply and hydroelectric energy production that had dramatic negative impacts on the Chilean economy (Donoso et al. 1999; Quintana 2000). Electricity and traffic signals were rationed for two hours per day. This resulted in monumental traffic jams in Santiago and severely curtailed economic activity (Rivas 1999; Maldonado 1999).

The instrumental precipitation record for Santiago de Chile is very long (1855–present) and it exhibits a

Corresponding author address: Carlos Le Quesne, Instituto de Silvicultura, Universidad Austral de Chile, casilla 567, Campus Isla Teja, Valdivia, Chile.
E-mail: clequesn@uach.cl

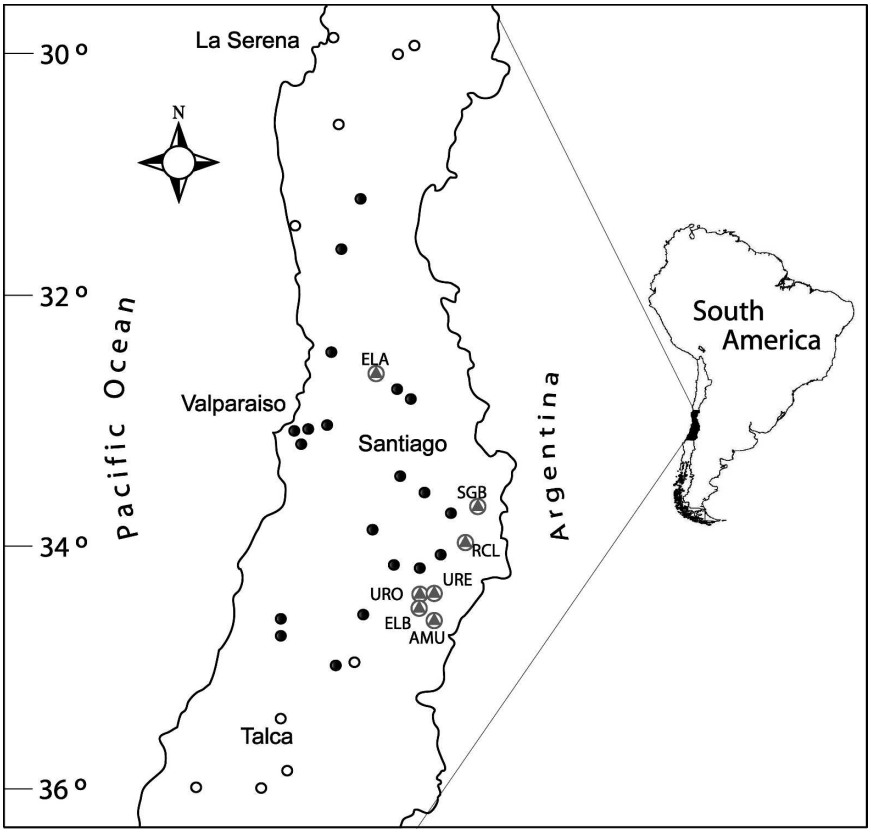

FIG. 1. This map locates the tree-ring chronology sites and instrumental precipitation stations investigated in central Chile. The stations noted with filled circles were used to compile the regional precipitation totals for central Chile, and open circles are stations not used (Table 1). The tree-ring site abbreviations are defined in Tables 2 and 3. *Austrocedrus* reaches the northern limit of its distribution at ELA.

modest secular decline in total annual precipitation (Luckman and Villalba 2001), much of which is associated with the apparently wetter conditions in the nineteenth and early twentieth centuries. The subsequent decline in Santiago precipitation during the twentieth century has been much less pronounced (Quintana 2004). However, dramatic and statistically significant reductions in annual precipitation have been detected in other long precipitation records from central Chile, including La Serena, Valparaiso, Concepción, and Valdivia (Quintana 2004). Given the sensitivity of the Chilean economy to water supply and hydroelectric power generation, a long-term perspective on the interannual, decadal, and lower-frequency variability of precipitation over central Chile would be very valuable.

The long-lived conifer *Austrocedrus chilensis* [(D. Don) Pic. Ser et Bizz.], commonly referred to as ciprés de la cordillera, is native to the Andean range of Chile and Argentina. *A. chilensis* reaches the arid northern limits of its distribution on the west side of the cordillera in central Chile [at El Asiento (ELA); Fig. 1], where it occurs in isolated populations near the tree line at elevations between 1600 and 2200 m. This species has clear annual growth rings that are sensitive to moisture supply, and individuals live for more that 1200 yr. For this study, we developed an expanded network of *A. chilensis* tree-ring chronologies in central Chile. We use the two longest and most precipitation-sensitive series to reconstruct a regional average of central Chile precipitation from A.D. 1200 to 2000 and compare drought and wetness conditions during the twentieth century with the previous seven centuries.

2. Data and methods

Monthly precipitation records were obtained for central Chile from Juan Quintana of the Dirección Meteorológica de Chile (DMC) and the office of the Dirección General de Aguas in Santiago (Quintana 2004). "Central" Chile is defined here to include the region of "Norte Chico" (latitude 30°–32°S) and the northern portion of the Mediterranean climate of Chile (latitude

TABLE 1. A listing of the instrumental precipitation stations from central Chile used in this analysis. These stations extend from ca. 30° to 36°S. The period of record is indicated, along with the source (DMC = Dirección Meteorológica de Chile; DGA = Dirección General de Aguas; and Quintana 2004). The eigenvector loadings for June–December precipitation from each station on the first (PC1) and second (PC2) principal components are also listed (analysis period = 1930–2000). All stations load positively on PC1, but note the polarity on PC2 and the sign change near 33°S. The 20 stations included in the regional average of June–December precipitation for central Chile are indicated with a double asterisk. The mean June–December precipitation for each station is also included.

Weather stations	Lat S, lon W	Elevation (m)	Full record	Jun–Dec average 1930–2000 (mm)	Source	PC1*	PC2*
La Serena	29°54′, 71°15′	30	1869–2000	68.2	DMC	0.1583	0.3486
Rivadavia	29°58′, 70°35′	820	1916–2000	87.6	DGA	0.1619	0.3043
Vicuña	30°02′, 70°44′	600	1918–2000	78.3	DMC	0.1507	0.3646
Ovalle	30°36′, 71°12′	220	1897–2000	95.2	DGA	0.1678	0.2889
Combarbalá**	31°11′, 71°02′	900	1922–2000	169.4	DMC	0.1853	0.2323
Puerto Oscuro	29°54′, 71°15′	10	1910–2000	98.9	DMC	0.1658	0.2034
Illapel**	31°36′, 71°11′	310	1913–2000	156.8	DMC	0.1671	0.2054
La Ligua**	32°27′, 71°16′	60	1912–2000	257.8	DMC	0.1941	0.1082
San Felipe**	32°45′, 70°44′	630	1925–2000	173.5	DMC	0.1906	0.1578
Los Andes**	32°50′, 70°37′	815	1907–2000	212.2	DGA	0.1924	0.0509
Limache**	33°01′, 71°18′	120	1918–2000	323.4	DMC	0.1937	0.0615
Valparaiso**	33°01′, 71°38′	40	1899–2000	296.0	DMC	0.1904	0.0504
Quilpue**	33°04′, 71°28′	100	1918–2000	315.1	DMC	0.1953	0.0255
Peñuelas**	33°10′, 71°32′	360	1915–2000	485.7	DGA	0.1950	−0.0005
Santiago**	33°27′, 70°42′	520	1866–2000	246.6	DMC	0.1958	−0.0093
La Obra de Maipo**	33°35′, 70°30′	800	1930–2000	495.2	DMC	0.1890	−0.1048
Queltehues**	33°49′, 70°12′	1360	1916–2000	519.1	DMC	0.1795	−0.1734
Aculeo**	33°53′, 70°55′	350	1913–2000	419.2	DMC	0.1893	−0.0871
Barahona Sitio K**	34°05′, 70°22′	1530	1921–2000	719.9	DMC	0.1804	−0.1925
Rancagua**	34°10′, 70°45′	500	1910–2000	315.2	DGA	0.1960	−0.0669
Coya**	34°12′, 70°33′	780	1922–2000	519.9	DMC	0.1899	−0.0851
San Fernando**	34°35′, 71°00′	350	1910–2000	549.4	DGA	0.1900	−0.1726
Pumanque**	34°37′, 71°40′	110	1930–2000	467.6	DMC	0.1955	−0.0963
Curicó**	34°59′, 71°14′	210	1918–2000	524.7	DMC	0.1893	−0.1505
Lolol**	34°45′, 71°40′	170	1919–2000	481.7	DMC	0.1901	−0.1470
Romeral	34°58′, 71°04′	200	1930–2000	496.5	DMC	0.1806	−0.1584
Talca	35°26′, 71°40′	100	1907–2000	488.0	DGA	0.1857	−0.1567
Linares	35°51′, 70°22′	160	1916–2000	644.2	DMC	0.1677	−0.2480
Cauquenes	35°59′, 72°22′	180	1919–2000	496.4	DMC	0.1724	−0.1463
Parral	36°09′, 71°50′	170	1918–2000	736.5	DMC	0.1638	−0.2688

* Eigenvector loadings for precipitation stations in the common period 1930–2000.
** Used for central Chile precipitation average.

32°–35°S). Records from 30 individual precipitation stations were evaluated in this analysis (Table 1). Some of these records extend back to the midnineteenth century, and all have the period 1930–2000 in common.

Seven annual ring width chronologies of *A. chilensis* (Table 2) from isolated outlying populations in central Chile have been compiled and updated for this analysis from the collections of LaMarche et al. (1979) and LeQuesne (1999). The *A. chilensis* tree-ring chronologies are among the most climate-sensitive in the Andes (Boninsegna 1992; Villalba 1994b) and in fact are the most long-lived precipitation-sensitive tree-ring chronologies currently known in the entire Southern Hemisphere. The *A. chilensis* populations sampled for this study were found near the arid northern latitudinal and upper altitudinal limits of the natural distribution of this species (Fig. 2). Both tree lines are controlled by aridity and available soil moisture, and the derived chronologies are highly correlated with seasonal precipitation totals across a broad section of central Chile. The tree-ring chronologies include core samples from living trees as much as 1200 yr old, and cross sections cut from relict wood still preserved in these very steep, rocky habitats. Vegetation cover is very low and the *A. chilensis* trees are widely separated due to the rocky and arid conditions (Fig. 2). Fires do occur but are limited, and of low intensity, which contributes to the preservation of valuable ancient *A. chilensis* wood (Aravena et al. 2003).

Core samples and cross sections of well-preserved subfossil wood were mounted and sanded according to the standard dendrochronological methods (Stokes and

TABLE 2. Tree-ring sites of *Austrocedrus chilensis* in central Chile (site codes are used in Fig. 1).

Site name and code	Lat S, lon W	Aspect	Elevation (m)	Dating	Number of tree-ring series
El Asiento, ELA	32°39′, 70°49′	S	1900–1700	955–2000	117
San Gabriel, SGB	33°46′, 70°14′	S	1550–1800	1131–1996	71
Rio Clarillo, RCL	33°49′, 70°25′	N	1700–2100	1204–2002	86
Urriola Este, URE	34°27′, 70°25′	E	1600–1700	1500–2001	75
Urriola Oeste, URO	34°27′, 70°26′	W	1600–1700	1205–2001	19
El Baule, ELB	34°29′, 70°26′	E	1800–1900	1149–2001	49
Agua de la Muerte, AMU	34°31′, 70°25′	W	1700–2000	1072–2001	108

Smiley 1996). The samples were visually cross-dated under the microscope (up to 50×) and tree-ring widths were measured to the nearest 0.01 mm with a stage micrometer. Cross dating was used to identify sequences of signature years (unique narrow and wide rings in specific chronological order) in the ring width series of all trees and radii from a given site (Fritts and Swetnam 1989; Kaennel and Schweingruber 1990). This procedure allows the detection of false and missing rings (both occur in this species, but infrequently) and the exact calendar year dating of all annual growth rings in each sample (Douglass 1941; Fritts 2001). The dating and measurement accuracy were checked with correlation analyses of 50-yr segments overlapped by 25 yr for each dated time series using the program COFECHA (Holmes 1983).

FIG. 2. A photograph of a drought-stressed *Austrocedrus chilensis* tree growing on a steep rocky slope at the Agua de la Muerte site in central Chile. This double-stem tree exhibits the classic characteristics of longevity in conifers (e.g., laterally twisted stems, crown die-back; Schulman 1956) and is 800 years old. This tree and others at the site record a detailed history of interannual and decadal drought episodes. Note the wide spacing of trees in the middle distance at this extremely arid site.

The chronologies cover the period A.D. 955–2000 and were standardized using the ARSTAN program (Cook and Holmes 1986). Standardization of the raw ring width series was accomplished by dividing the tree-ring width in year t by the year t value of a negative exponential curve, or, if the exponential could not be fitted, a linear regression line with negative slope was fitted to the time series (Fritts 2001). The ring width indices from this "first detrending" operation were then again detrended in a second operation where an inflexible smoothing spline was fit to each ring width index time series (Cook and Peters 1981). These procedures are intended to remove the biological age trend in radial growth (Fritts 2001), and the general absence of temporal coherence between the smooth detrending curves fit to each component ring width time series supports the interpretation that the low-frequency variability was not of climatic origin. The overwhelming majority of all individual ring width time series were detrended with a negative exponential curve, which is the classic model for the age- and size-related decline in average radial growth in trees (Fritts 2001).

3. Central Chile precipitation and the growth of *Austrocedrus chilensis*

The Mediterranean climate zone of central Chile is transitional between the hyperarid midlatitude deserts of northern Chile and the wet marine west coast climate

to the south (Miller 1976). The summer dry climate of this region is characterized by highly variable winter and spring precipitation, with severe droughts and frequent floods (Almeyda 1948; Ortlieb 1994, 2000). The interannual variability of precipitation over central Chile is partially associated with El Niño–Southern Oscillation (ENSO; Aceituno 1988). During El Niño episodes there is a tendency for above-average winter precipitation, while La Niña events are often associated with drought (Rutlland and Fuenzalida 1991; Montecinos and Aceituno 2003).

The first instrumental measurement of precipitation in central Chile began in 1855 at the observatory on Cerro Santa Lucia in the city of Santiago by Ignacio Domeyko in association with an astronomical expedition to Chile by J. N. Gillis (Gillis 1855). The recording station was relocated to Quinta Normal in 1866, where daily precipitation observations have continued largely unbroken to the present. The precipitation observation network in Chile now includes some 50 stations with at least 50 yr of record (e.g., Quintana 2004).

A number of interesting analyses of precipitation variability across the entire 38° latitudinal range of Chile have been reported, including the classic studies of Taulis (1934) and Van Husen (1967), and the recent work of Montecinos and Aceituno (2003). An estimated 90% of the moisture in central Chilean precipitation is associated with wave activity in the westerlies, with the remaining 10% associated with cutoff cyclones of Pacific origin (Montecinos and Aceituno 2003). The circa 5000-m average elevation of the Andes Cordillera effectively prevents the intrusion of Atlantic moisture westward into central Chile (Montecinos and Aceituno 2003).

Van Husen (1967) and Montecinos and Aceituno (2003) have both analyzed the spatial distribution of precipitation over Chile. Montecinos and Aceituno (2003) used principal component analysis (PCA) of winter (June–August) precipitation totals and identified central Chile as a homogeneous precipitation province extending from 30° to 35°S. Our analysis of 30 selected high-quality precipitation records from central Chile confirms their conclusions. PCA of these 30 stations for various seasonal totals (e.g., May–September and June–December) indicate very strong eigenvector loadings by all individual stations on the first principal component (Table 1), which in the case of the June–December season explains 70% of the overall variance in the 30 stations. The eigenvector loadings on the second principal component indicate a sharp north–south gradient in precipitation (Table 1), as described by Van Husen (1967) based on precipitation amounts delivered in individual storm events. The change point in this gradient is located just south of Santiago in both the analysis of Van Husen (1967) and our PCA of June–December precipitation totals. This inflection point essentially separates the region of episodic dry winters to the north from more southerly climates that always receive at least some precipitation during the winter (Van Husen 1967).

We used correlation analysis to identify the region of central Chile where precipitation has the strongest relationship with tree growth, and to define the strongest seasonal precipitation response of the *A. chilensis* tree-ring chronologies. All 30 instrumental precipitation records from central Chile (Table 1) are significantly correlated ($P < 0.05$) with our tree-ring chronologies, but the 20 stations closest to the chronologies had the highest correlations with tree growth. We used these 20 stations to develop an instrumental monthly precipitation average for central Chile extending from 1930 to 2000 (the 20 stations are indicated in Table 1 and Fig. 1). This regional precipitation average extends from the southern edge of Norte Chico near Combarbalá south into the true Mediterranean climate close to Talca. The June–December seasonal total precipitation amounts range from 157 mm in the north at Illapel to 720 mm at Barahona (Table 1), and they average 384 mm for the study area.

All tree-ring chronologies are significantly correlated with winter–spring precipitation over central Chile, but the El Asiento and El Baule chronologies had the best correlations and were averaged into a single regional time series of tree growth for long-term reconstruction. These two chronologies are well correlated over their entire 800-yr interval used for reconstruction ($r = 0.47$; $p < 0.001$), and over the period of observed data when they are best replicated ($r = 0.63$, $p < 0.0001$). The two chronologies capture most of the spatial variability evident in a PCA of the seven available tree-ring chronologies (Table 3). All seven chronologies are significantly cross correlated (all with $p < 0.0001$) and load strongly on the first PC (Table 3). On the second PC, the three northernmost chronologies load positively (including El Asiento) and the four southern chronologies load negatively (including El Baule). These spatial patterns of tree growth are very similar to the precipitation patterns, and the change point in these eigenvector loadings is located in the same vicinity as the change point for the second PC loadings for June–December precipitation.

Correlation analysis was used to define the principal seasonal response of *A. chilensis* in central Chile. The regional average of El Asiento and El Baule (hereafter referred to as the tree-ring chronology) was correlated

TABLE 3. Eigenvector loadings for PC1 and PC2 of tree growth (computed on the tree-ring chronologies for the common period from 1500 to 1996). The principal component loadings for the tree-ring sites are similar to the spatial patterns observed for the precipitation stations. The three northern chronologies load positively on PC2.

Site name and code	Lat, S	PC1	PC2
El Asiento, ELA	32°39′	0.3211	0.7708
San Gabriel, SGB	33°46′	0.3720	0.0397
Rio Clarillo, RCL	33°49′	0.3663	0.3806
Urriola Este, URE	34°27′	0.3883	−0.2290
Urriola Oeste, URO	34°27′	0.3809	−0.2652
El Baule, ELB	34°29′	0.4047	−0.2567
Agua de la Muerte, AMU	34°31′	0.4057	−0.2660

with monthly precipitation totals for central Chile for the period 1930–2000 (Fig. 3). The tree-ring chronology is significantly correlated ($p \leq 0.05$) with precipitation from June through November (Fig. 3), the period just prior to and including the growing season of *A. chilensis* in central Chile (typically September–December). Even though the correlation is low, we included December in the seasonal precipitation average because *A. chilensis* may still be influenced by unusual rainfall events late in the growing season.

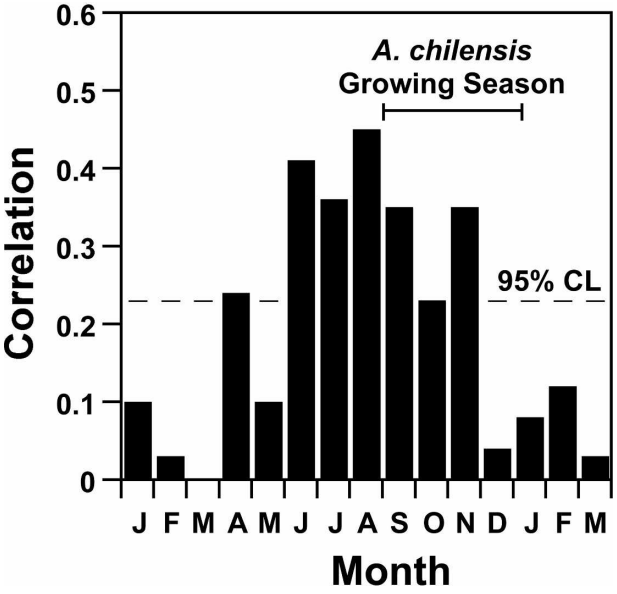

FIG. 3. The seasonal precipitation response of the regional average *Austrocedrus chilensis* tree-ring chronology was defined using correlation analysis, comparing the chronology with monthly precipitation totals in the 20-station regional average for central Chile. The growing season of *A. chilensis* typically begins in September and ends in December or early January, but radial growth is strongly influenced by precipitation amounts both during and immediately preceding the growing season ($P < 0.05$). The strongest response of *A. chilensis* to precipitation occurs during the principal JJA winter wet season in central Chile.

4. Results

The regional average of the El Asiento and El Baule tree-ring chronologies was used to estimate the 20-station regional average of June–December precipitation for central Chile. Because there is also no significant low-order autocorrelation in the regional average of June–December precipitation for central Chile (autoregressive modeling identified the time series as a white noise process, i.e., AR-0), white noise versions of the El Asiento and El Baule series were used to develop the regional tree-ring chronology (this chronology is also not normally distributed, and skewness = 0.77 for the period 1930–2000). The central Chile precipitation series [$\hat{Y}$ in Eq. (1)] extends from 1930 to 2000 and is not normally distributed (modestly skewed by a few years of very heavy precipitation, skewness = 0.92; Fig. 4). In an attempt to better estimate these heavy precipitation extremes, the June–December precipitation series was transformed with the natural logarithm function prior to calibration modeling with tree growth. There was judged to be a marked improvement in the relationship created by the transformation, based on a 10% increase in variance explained for 1930–2000 (Table 4a). The calibration bivariate regression model used to reconstruct June–December precipitation was

$$\ln \hat{Y} = 4.104 + 1.737\, X_t, \quad (1)$$

where $\ln \hat{Y}_t$ is the natural-log-transformed estimate of June–December precipitation for central Chile in year t

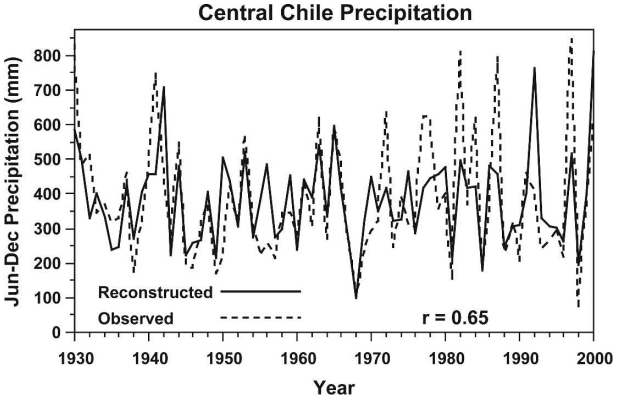

FIG. 4. The instrumental and reconstructed June–December precipitation totals for central Chile are plotted from 1930 to 2000. The calibration [Eq. (1)] was based on the natural-log-transformed version of the instrumental precipitation series from 1965 to 2000 (back-transformed using general linear modeling), and verified from 1930 to 1964 (Table 3). Here the instrumental and reconstructed data are plotted in real units of precipitation (mm), and the correlation between the two series from 1930 to 2000 is $r = 0.65$ ($P < 0.001$). Note the increase in positive precipitation extremes after 1980, and the tendency for ≥2 consecutive years of below average precipitation in both time series.

TABLE 4a. The calibration used the regional average of the El Asiento and El Baule persistence-free (AR-0) chronologies as the predictor with two different predictands, 1) the natural-log-transformed June–December total precipitation [used for the reconstruction; see Eq. (1)] and, 2) the untransformed average June–December precipitation (for comparison purposes only). The statistics (Draper and Smith 1981) calculated for the calibration period were the R^2 adjusted for loss of degrees of freedom, tests of difference from 0.0 of the regression coefficients, and the Durbin–Watson statistic of autocorrelation in the residuals from regression, a test of the aptness of the model.

Period	R^2_{Adj}[a]	Coefficient		Standard error (mm)		T statistic (H_0: $\beta=0$)		Regression[b] residual autocorrelation
		β_0	β_1	β_0	β_1	β_0	β_1	
ln transformed predictand, model used for reconstruction [see Eq. (1)]								
1930–2000	0.55	4.104	1.737	0.189	0.185	21.7[c]	9.4[c]	−0.13NS[d]
Predictand not transformed								
1930–2000	0.45	−199.0	582.1	77.48	75.98	−2.6[e]	7.7[c]	−0.12NS
ln transformed predictand								
1930–64	0.44	4.388	1.458	0.282	0.277	15.6[c]	5.1[c]	0.10NS
1965–2000	0.61	3.928	1.909	0.260	0.254	15.1[c]	7.5[c]	−0.23NS

[a] R^2 adjusted downward for loss of degrees of freedom (Draper and Smith 1981).
[b] Autocorrelation of the residuals from regression, tested with the Durbin–Watson statistic (Draper and Smith 1981). Failure to reject the null hypothesis indicates that the residuals occur randomly, an indication that the regression model is valid.
[c] Significant, $p < 0.001$.
[d] NS: not significant; i.e., there is >5% probability that the result occurred by chance.
[e] Significant, $p < 0.05$.

and X_t is the regional average tree-ring chronology in year t. Then ln $\hat{Y}_t$ was back transformed into the original units of precipitation to complete the reconstruction of June–December precipitation ($\hat{Y}$) in millimeters. The back transformation was accomplished as follows (J. Dunn 2005, personal communication; Like 1980):

$$\hat{Y} = [\exp(\beta_1 X)]\,\{\exp[(\mathrm{MSE})(1 - H)/2]\}, \qquad (2)$$

where $\hat{Y}$ is the back transform of estimated natural logarithm of precipitation; exp is the function that raises the natural logarithm base, e (~2.71828), to the specified power; β_1 X is the estimate of transformed climate from the tree-ring variable, X, and the regression coefficient, β_1; MSE is the mean-squared error estimated in regression (Draper and Smith 1981); and H is defined as the vector of individual annual estimates of leverage, $h_i = x_i\,(\mathbf{X'X}) - 1\,x_i'$ [Computed for all X_t in the SAS general linear modeling procedure (GLM); SAS Institute, Inc. 1999]. Leverage is a measure of how influential the predictor is in regression.

The regional precipitation series was also split into two subperiods (1930–64 and 1965–2000), and calibration was performed in these additional periods as a means of validating the regression model (Snee 1977). The regression coefficients in the subperiods were compared and found to be not significantly different. The verification statistics were then calculated by comparing the estimated and instrumental time series in original units (Table 4b). The subperiod verification statistics and similar coefficients justify our decision to use all the observations (1930–2000) to generate the model used for reconstruction [Eq. (1)], although the regression relationship is not as good for 1930–64 as it is for 1965–2000.

The time series of instrumental and reconstructed June–December precipitation (in millimeters) are plotted from 1930 to 2000 in Fig. 4. The entire 801-yr reconstruction is plotted from A.D. 1200 to 2000 in Fig. 5. The tree rings explain 55% of the variance in the log-transformed June–December precipitation series (R^2adj = 0.55) and 45% of the variance in the untransformed precipitation during the full calibration period (Table 4a). The residuals from regression do not exhibit significant trend [based on the Durbin–Watson test statistic (Draper and Smith 1981); Table 4a], a further validation of the model.

The verification statistics indicate that the reconstructions from both transformed and untransformed precipitation are doing a good job of estimating the instrumental June–December precipitation for central Chile (Table 4b). All verification tests on independent instrumental June–December precipitation data for central Chile are passed, including the reduction of error (RE) and coefficient of efficiency (CE) tests, which are considered quite stringent (Cook and Kairiukstis 1990; Fritts 2001). Both versions of the reconstruction are well correlated (r) with the instrumental precipitation data during the verification periods (including first-differenced versions of the time series; Table 4b). The

TABLE 4b. Verification of the two subperiod calibrations (1930–64 and 1965–2000) in Table 4a. The 1930–64 subperiod calibration is verified independently by observed data for 1965–2000 and vice versa for the 1965–2000 calibration. The statistics calculated for the verification period are Pearson correlation coefficient *r*, correlation of first differenced series, sign test, paired *t* test, RE, and CE. Both subperiod reconstructions pass all statistical tests in the verification periods [see Cook and Kairiukstis (1990) for further details on the verification statistics], indicating that the full period calibration, 1930–2000, should be statistically valid.

Period	Pearson correlation	First diff[a] correlation	Paired *t* test[b] of mean (*t* value)	Sign test[c] (hit/miss)	RE[d]	CE[e]
1930–64 (Calibrated 1965–2000)	0.67[f]	0.56[f]	−0.56NS[g]	29/7[f]	0.38	0.37
1965–2000 (Calibrated 1930–64)	0.76[f]	0.86[f]	0.53NS	27/8[f]	0.44	0.44

[a] Observed and reconstructed data first differenced ($t - t_{-1}$). The transformation removes trends that may affect the Pearson correlation coefficient (Fritts 2001).
[b] Paired comparison of observed and reconstructed data means (Steel and Torrie 1980). Note that no difference is the desired result.
[c] Signs of departures from the mean of each series (Fritts 2001). Means are subtracted from each series and the residuals are multiplied. A positive product is a "hit." If either observed or reconstructed data lie on the mean, the year is omitted from the test.
[d] There is no formal test of significance for this statistic, which ranges from $-\infty$ to $+1$, but any positive result indicates that the reconstruction contributes unique paleoclimatic information (Cook and Kairiukstis 1990; Fritts 2001).
[e] This is a somewhat more stringent test than the RE. Again there is no formal test of significance, but if it is positive and not much less than the RE, that indicates a satisfactory reconstruction (Cook and Kairiukstis 1990).
[f] Significant, $p < 0.001$.
[g] NS: Not significant, i.e., >5% probability that the result occurred by chance.

sign test indicates that the sign of departures above and below the mean for instrumental and reconstructed precipitation are usually in agreement during the verification period ($p < 0.001$), and the means of the estimated and observed series are not significantly different (paired *t* test, $p < 0.01$; Table 4b).

The time series comparisons in Fig. 4 indicate that the reconstruction is most accurate in estimating drought conditions, including 1938, 1949, 1968, 1981, and 1998, the five driest years in the instrumental precipitation series for central Chile since 1930. However, the increase in extremely wet years after 1980 is not well estimated by the tree-ring reconstruction (Fig. 4), in spite of the natural log model [Eqs. (1) and (2)].

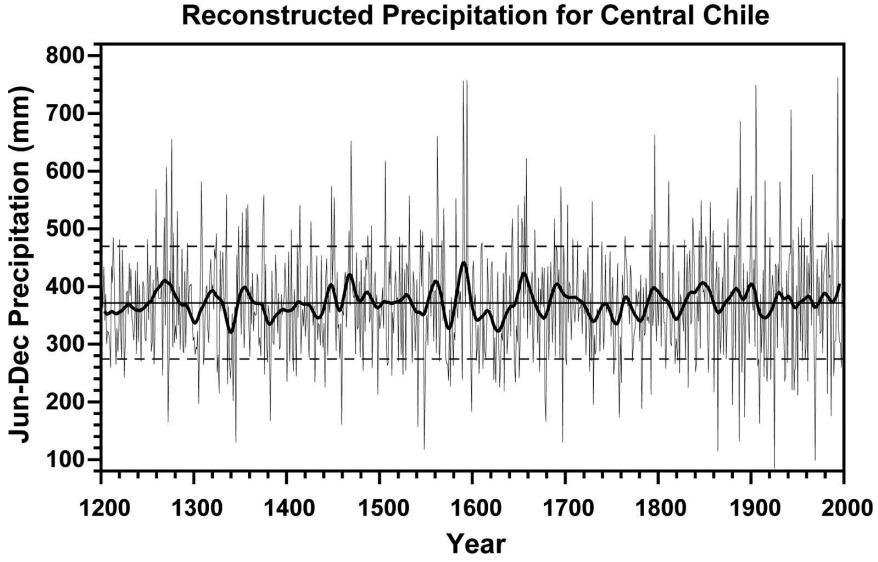

FIG. 5. Tree-ring reconstructed June–December precipitation for central Chile extends from A.D. 1200 to 2000. A cubic smoothing spline highlighting multidecadal variability (ca. 25 yr, fit for the period 1205–1995) and the ±1.0 std dev thresholds are also plotted. The reconstruction indicates that multidecadal variability was greater at times prior to the twentieth century, and that the nineteenth century was wetter than the twentieth century.

5. Analysis of reconstructed precipitation for central Chile

The tree-ring reconstruction of June–December precipitation for central Chile is plotted in Fig. 5 along with a 25-yr smoothing spline to emphasize multidecadal variability and the ±1.0 standard deviation thresholds. The reconstructed time series has no significant low-order autocorrelation and is modeled as a white noise autoregressive process (AR-0). The full 801-yr-long reconstruction is not normally distributed with slight positive skewness (skewness = 0.59), which underestimates the skewness computed for the instrumental precipitation data from 1930 to 2000 (skewness = 0.92), probably because the tree-ring data do not reproduce well the wettest extremes (Fig. 4). The reconstruction is dominated by high-frequency interannual variability over the last 800 yr, but there is an increase in the envelope of variability after circa 1850, including estimates of more frequent extreme drought and wet years (Fig. 5).

Figure 5 suggests that the decadal variability of central Chile precipitation was greater before the twentieth century, with more intense and prolonged dry and wet episodes. Note particularly the multiyear drought episodes of the eighteenth, seventeenth, sixteenth, and fourteenth centuries, which exceed the estimates of decadal drought during the twentieth century (Fig. 5). In fact, historical climate references provide some independent confirmation of drought conditions during the seventeenth and eighteenth centuries. Prolonged dry conditions are estimated during the early seventeenth century (Fig. 5), which includes "La Sequía de San Juan de Mañosca" from 1636 to 1639 (Vicuña Mackenna 1877; Bonilla 1999; Piwonka 1999) when three of the four years are estimated to have had below-average precipitation (i.e., 285.5, 313.4, 335.9, and 421.0 mm for 1636–39, respectively, and an estimated 801-yr June–December mean precipitation of 372.1 mm). Historical data compiled by Vicuña Mackenna (Vicuña Mackenna 1877; Taulis 1934) also indicate intense decade-long drought in the 1770s and early 1780s, as reconstructed for central Chile from cypress trees (Fig. 5) when 10 of the 15 yr from 1771 to 1785 are estimated to have had below-average precipitation and the 15-yr reconstructed mean precipitation only was 332.9 mm, relative to an estimated 801-yr average of 372.1 mm. Periods of reduced decadal variability like the twentieth century are also seen in the reconstruction 1200–60, 1380–1420, and 1480–1530. The cause is not known and it may be a random effect.

The historical references we have found provide little evidence for the multidecadal wet regimes reconstructed for central Chile (Fig. 5; historical references to wet periods may be lacking because people are more negatively affected by drought), but the terminus of the Rio Cipreses glacier has been in massive retreat since the midnineteenth century (C. Le Quesne et al. 2006, unpublished manuscript). This glacier is located near the Agua de la Muerte cypress site some 80 km south of Santiago. The 1842 position of the terminus was located some 4.5 km down valley from its present position, during a reconstructed multidecadal wet episode that may have been unmatched in 300 yr (Fig. 5). Cobos and Boninsegna (1983) also documented the early-nineteenth-century wet period in the Rio Atuel River basin (1820–50) using tree-ring data, including an earlier version of the El Asiento chronology.

Careful inspection of the observed and reconstructed June–December precipitation data suggest a regime-like behavior to drought episodes in central Chile, with many consecutive runs of below-mean precipitation observations and estimates. We used the Lilliefors Interval Exponential Distribution Test (Conover 1980) to evaluate the statistical significance of this apparent nonrandom clustering of drought years. We defined "drought" with a threshold of ≤0.5 standard deviations below the mean (88.94 mm for the instrumental and 48.39 mm for the reconstructed data). Using these thresholds, the frequency of 1-yr intervals between droughts (consecutive drought years) is higher than expected from a random exponential distribution of intervals in the instrumental precipitation data (1930–2000; $p \leq 0.01$) and for 1-, 2-, and 3-yr intervals in the reconstruction (1200–2000; $P \leq 0.01$). These regimes may arise in part from the slight skewness in both time series but nevertheless may have some modest value for probabilistic forecasting of drought.

The reconstruction also suggests that the probability of drought exceeding the −1.0 standard deviation threshold changes substantially over time. We used return time analysis to examine the changing risk of drought over the past 800 yr. The risk of experiencing a drought of given magnitude can be computed from the overall probability of occurrence for that drought threshold in the available record (Viessman et al. 1972). Here we compute the risk or "return time" probabilities for seven thresholds of below-average precipitation in central Chile, using the 71-yr-long instrumental and 801-yr-long reconstructed records (Fig. 6). Because the regression-based reconstruction underestimates the instrumental departures during the calibration period, we first adjusted the reconstructed risk (1200–2000) for each return interval (2 to 99 intervals) and each of the seven thresholds of drought (7 × 99 for 693 adjustments) by the ratios of observed to reconstructed risk

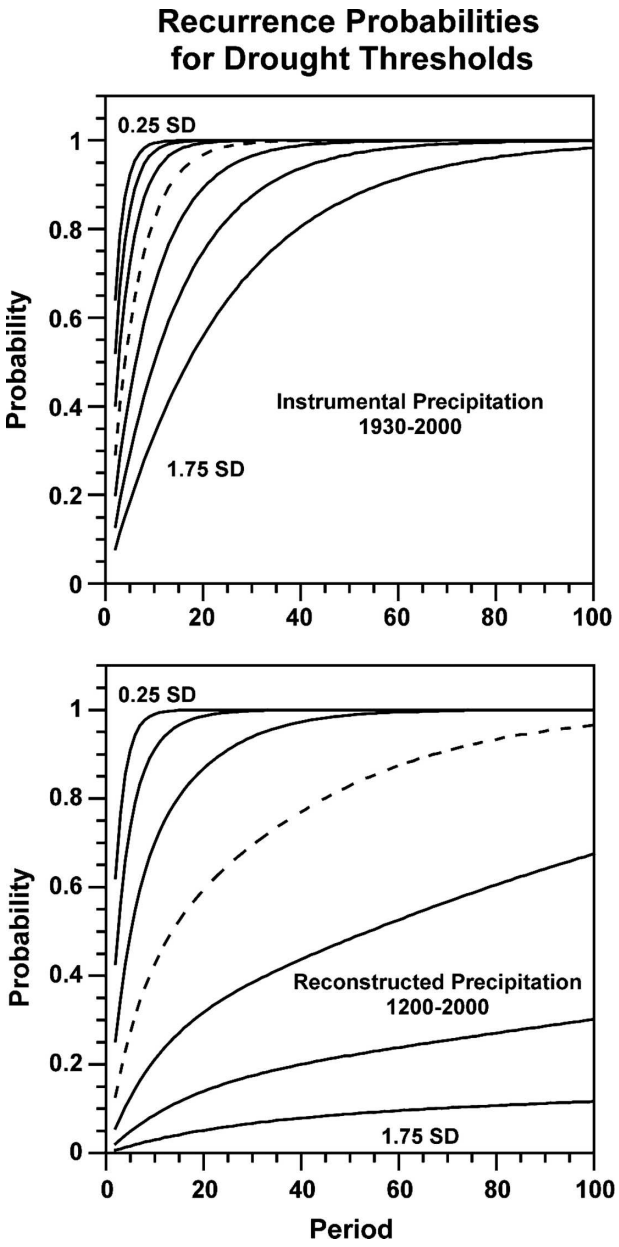

FIG. 6. Return time analyses computed for the (top) instrumental (1930–2000) and (bottom) adjusted tree-ring reconstructed (1200–2000) central Chile precipitation time series. Return time was computed for seven thresholds of drought severity (0.25, 0.50, 0.75, 1.0, 1.25, 1.50, and 1.75 std devs) and for return periods from 2 to 99 yr. The lowest threshold (0.25) is plotted at the far left in both figures. The return time for a drought ≤1.0 std dev below the mean is indicated by the dashed line in both plots, and the 50% probability for this level of drought increases from (bottom) once in 13 yr in the reconstructed series to (top) once in 4 yr in the instrumental series.

during the period in common to both time series (1930–2000) on the assumption that this adjustment would be constant through time.

The risk of drought in all severity classes has increased during the twentieth century (i.e., the return time has shortened), when compared with the past 800 yr (Fig. 6; Table 5). For example, in the instrumental record for central Chile (1930–2000) there is about a 50% probability for a drought event ≤1.0 standard deviation below the mean (382.4 − 177.9 = 204.5 mm) to recur in only 4 yr, but that same threshold of drought recurred in 13 yr when computed on the 801-yr reconstruction (1200–2000). In fact, when the return intervals for drought are computed for all nonoverlapping 71-yr-long time intervals from 1220–2000, the 50% recurrence probability for a drought ≤1.0 standard deviation below the mean ranges from a low of 48 yr (1433–1503; Table 5) to a high of 4 yr (both 1859–1929 and 1930–2000; Table 5). Only one reconstructed 71-yr interval during the past 800 yr has approached the high drought risk of the late nineteenth and twentieth centuries, the period from 1575 to 1645 when the 50% recurrence probability for a drought ≤1.0 standard deviation below the mean increased to only 7 yr (Table 5).

So in spite of major differences in the methods used to develop the tree-ring chronologies (we used conventional methodology to detrend and AR model the ring width data; cf. Fritts 2001; Cook 1985), our analysis confirms the increasing vulnerability to drought in central Chile during the twentieth century suggested

TABLE 5. The approximately 50% recurrence probabilities for drought ≤1.0 std dev below the mean are listed in years for the instrumental (1930–2000) and adjusted reconstructed (1200–2000) precipitation series for central Chile (with their time interval, mean and std dev), and for 11 nonoverlapping 71-yr intervals reconstructed from 1220 to 2000 (for comparison with the twentieth century). Note the high risk of drought (short intervals) computed for the instrumental precipitation series and for the reconstructed series during the late nineteenth–twentieth centuries (1859–1929, 1930–2000) and in the late sixteenth–early seventeenth centuries (1575–1645).

Span	Mean (mm)	Std dev (mm)	Return interval, $P = \sim 0.50$ of −1 std dev drought
Instrumental			
1930–2000	382.4	177.9	4
Adjusted reconstructed			
1200–2000	372.1	96.8	13
1930–2000	383.7	32.8	4
1859–1929	370.2	121.0	4
1788–1858	384.1	91.4	32
1717–87	355.5	73.7	46
1646–1716	383.8	93.7	27
1575–1645	362.7	104.3	7
1504–74	374.4	99.6	12
1433–1503	378.3	83.8	48
1362–1432	360.7	78.4	38
1291–1361	367.6	90.1	19
1220–90	375.2	88.5	29

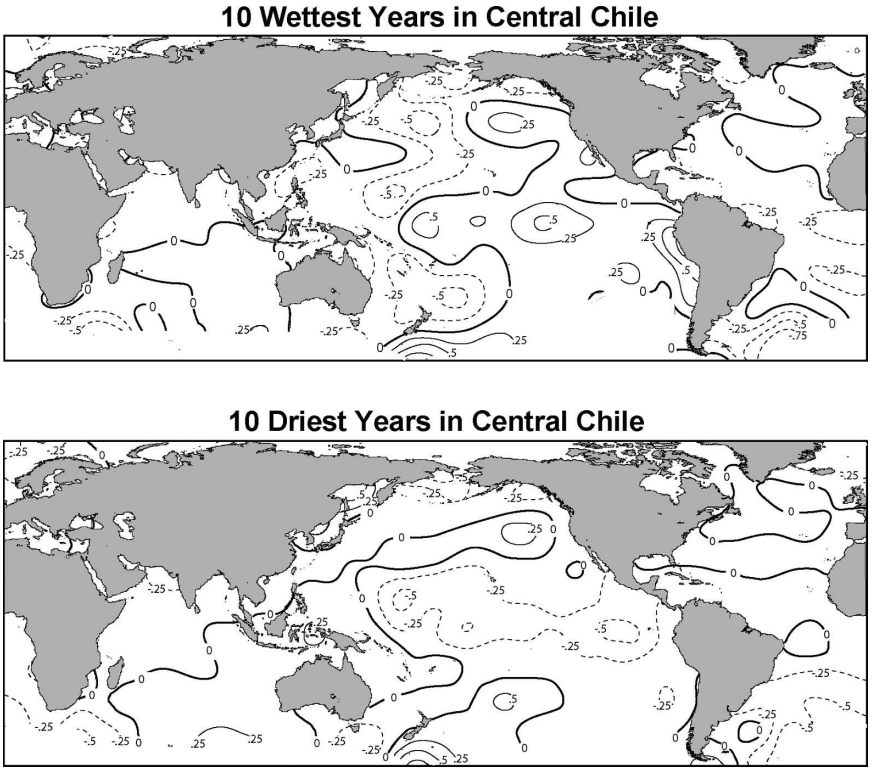

FIG. 7. Composite winter wet season (JJA) SST maps of anomalies from the 1951–80 mean (Kaplan et al. 1998) for the 10 wettest (in order: 1899, 1884, 1930, 1914, 1965, 1887, 1942, 1904, 1992, 2000) and the 10 driest years (in order: 1924, 1968, 1863, 1886, 1908, 1892, 1985, 1998, 1879, 1949) in the June–December precipitation reconstruction for central Chile from 1856 to 1991. Note the warm El Niño conditions, including warm conditions along the west coast of South America during the wettest years, and the cold La Niña conditions during the driest years.

by the studies of Boninsegna (1988) and Luckman and Villalba (2001). In our analysis this is due in part to the overall increase in the envelope of reconstructed precipitation variance in the past 150 yr (Fig. 5; Table 5).

The interannual variability of precipitation at Santiago has been linked in part to the ocean and atmospheric circulation changes associated with ENSO (Quinn and Neal 1983; Rasmusson et al. 1990; Rutlland and Fuenzalida 1991; Villalba 1994a), and the regional average of June–December precipitation in central Chile is correlated with the June–August (JJA, hereafter 3-month periods are denoted by the first letter of each respective month) average Southern Oscillation index (SOI; Jones 2005) at $r = 0.60$ ($p < 0.001$) from 1930 to 2000. Analyses of the reconstruction provide some support for an ENSO influence on central Chile precipitation and tree growth. Reconstructed June–December precipitation is correlated with the JJA SOI at $r = 0.31$ ($p < 0.01$) for the period 1855 to 2000. A composite analysis of the global sea surface temperature (SST) field (Kaplan et al. 1998) during the 10 wettest and 10 driest estimates of central Chile precipitation from 1866 to 1991 is presented in Fig. 7. The strongest SST anomalies associated with drought or wetness extremes over Chile were observed for the JJA season concurrent with winter precipitation (Fig. 7), with anomalously warm conditions in the eastern equatorial Pacific during wet extremes (El Niño events) and cold conditions in the same region during dry extremes (La Niña events). Midlatitude SST gradients in the South Pacific were also present during these Chilean moisture regimes (Fig. 7). Similar, though weaker SST patterns were observed in composite maps for the other seasons (e.g., DJF and MAM prior to the winter wet season in Chile; not shown).

Spectral analysis (Jenkins and Watts 1968) of the 801-yr reconstruction indicates modest spectral power ($p < 0.05$) in the ENSO frequency band (Rasmusson et al. 1990; Fig. 8) that cumulatively represents some 11% of the variance in the time series (i.e., the sum of spectral peaks between periods of 2.75 and 3.45 yr that exceed the 95% confidence limit; Fig. 8). The recon-

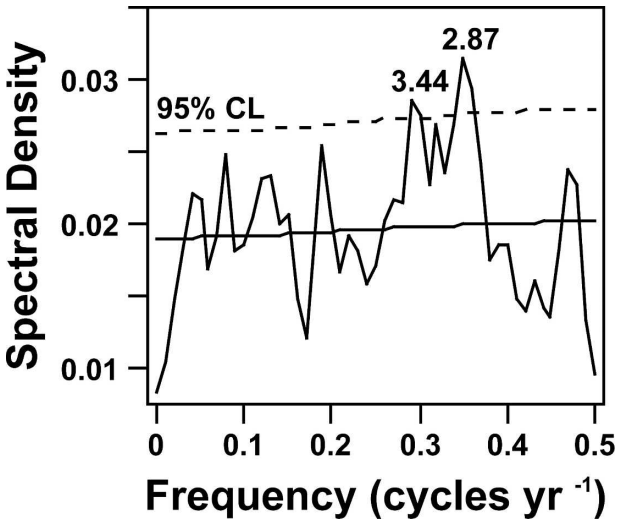

FIG. 8. The spectral density function calculated on the 801-yr reconstruction of central Chile precipitation has modest spectral power in the ENSO frequency band (spectral peaks exceeding the 95% confidence limit occurred at periods of 2.78, 2.87, 3.33, and 3.44 yr). A Hamming window with a bandwidth of 0.0252, 40 degrees of freedom, and 50 lags in estimating the autocorrelation function was used to compute the spectrum (IMSL 1982).

structed precipitation series also exhibits coherence with the instrumental precipitation series for central Chile (1930–2000) and with the SOI (1866–2000) at these same ENSO frequency bands ($P < 0.05$; not shown). This evidence for ENSO time-scale influences on central Chile precipitation suggests that some of the short interval regime-like behavior of instrumental and reconstructed precipitation may arise from persistent warm and cold events in the equatorial Pacific.

6. Conclusions

The instrumental precipitation records from central Chile, including La Serena and Santiago, are among the longest available for the Southern Hemisphere and indicate a pronounced drying trend from the mid- to late nineteenth century to the present (Houghton et al. 2001; Quintana 2004). These long-term moisture regime changes are supported by proxy indicators such as the retreat of the Rio Cipreses glacier from 1842 until the present in central Chile, near the location of the Agua de la Muerte tree-ring chronology (C. Le Quesne et al. 2006, unpublished manuscript).

The instrumental 20-station regional average of June–December precipitation totals for central Chile do not exhibit any statistically significant trend in the mean for the period 1930 to 2000 (Fig. 4). The new tree-ring reconstruction of June–December precipitation also does not exhibit the dramatic decline in growth and inferred precipitation noted during the late twentieth century for the El Asiento site by Boninsegna (1988) and Luckman and Villalba (2001), partly due to the radical differences in the methods used to detrend the ring width data. Nevertheless, the new precipitation reconstruction (Fig. 5) does indicate that the nineteenth century was slightly wetter than the twentieth century in central Chile (e.g., the reconstructed mean June–December precipitation from 1821 to 1905 was 390.4 mm and from 1906 to 2000 it was 375.8 mm, an estimated decline of 3.7%). The reconstruction also indicates greater decadal variability before 1900 and an increase in interannual variability after 1850 (Fig. 5). In fact, the risk of drought exceeding all thresholds increases dramatically in the reconstructed precipitation series after 1850, consistent with the drying trends indicated by selected long instrumental precipitation records, and by previous studies of tree growth and glacial recession. The practical significance of this reconstructed increase in drought risk for water resource management in central Chile is potentially enormous in light of the expanding agricultural, industrial, and municipal demands on water supply and hydroelectric power generation (Donoso et al. 1999).

The degree to which the short-term regimes and multidecadal trends noted in central Chile precipitation might be influenced by dynamic or purely stochastic factors remains to be determined. Future dendroclimatic research on the developing latitudinal array of moisture-sensitive cypress chronologies distributed west of the Andean Cordillera from central to south-central Chile will help test hypotheses about the spatial structure of Chilean drought and wet periods and their possible forcing by large-scale circulation regimes.

Acknowledgments. This research was supported by Conicyt Chile through Grant FONDECYT 3020011, by the U.S. National Science Foundation (Grant ATM-0400713), and the Inter-American Institute for Global Change Research (Americas Treeline Environments Grant CRN03). We were assisted in the field by Julio Cesar Vergara, Carlos Peña, Pedro Berhó, and Mauricio Fuentes, and in the laboratory by R. D. Griffin and Falko K. Fye. We thank Dr. James E. Dunn, University of Arkansas Emeritus Professor of Statistics, for statistical assistance, and two anonymous reviewers. We thank Juan Quintana and Carlos Valdes for facilitating the acquisition of precipitation data. And CLQ would also like to thank for the postdoctoral fellowship on the Millennium Nucleus P01-051-F of the Universidad Austral de Chile.

The ring width data and final chronologies from El

Asiento and El Baule, along with the instrumental central Chile precipitation average and the reconstruction, have been contributed to the International Tree-Ring Data Bank at the NOAA/National Climatic Data Center (http://www.ncdc.noaa.gov/paleo/).

REFERENCES

Aceituno, P., 1988: On the functioning of the Southern Oscillation in the South American sector. Part I: Surface climate. *Mon. Wea. Rev.,* **116,** 505–524.

Almeyda, E., 1948: *Rainfall of the Desert Zones and the Warm Steppes of Chile* (in Spanish). Editorial Universitaria, 162 pp.

Aravena, J. C., C. LeQuesne, H. Jiménez, A. Lara, and J. J. Armesto, 2003: Fire history in Central Chile: Tree-ring evidence and modern records. *Fire and Climatic Change in Temperate Ecosystems of the Western Americas,* T. T. Veblen et al., Eds., Springer-Verlag, 343–356.

Bonilla, C., 1999: Drought in Chile: Historical context and consequences in the agro-silvo-pastoral sector. *Drought in Chile: Causes, Consequences and Amelioration* (in Spanish), A. Norero and C. Bonilla, Eds., Pontificia Universidad Católica, 15–22.

Boninsegna, J. A., 1988: Santiago de Chile winter rainfall since 1220 as being reconstructed by tree rings. *Quat. South Amer. Antarct. Peninsula,* **6,** 67–87.

——, 1992: South American dendrochronological records. *Climate Since A.D. 1500,* R. S. Bradley and P. D. Jones, Eds., Chapman and Hall, 446–462.

Cobos, D. R., and J. A. Boninsegna, 1983: Fluctuations of some glaciers in the upper Atuel River basin, Mendoza, Argentina. *Quat. South Amer. Antarct. Peninsula,* **1,** 61–82.

Conover, W. J., 1980: *Practical Nonparametric Statistics.* 2d ed. John Wiley & Sons, 493 pp.

Cook, E. R., 1985: A time series analysis approach to tree-ring standardization. Ph.D. dissertation, University of Arizona, 171 pp. [Available from ProQuest Co., 300 N. Zeeb Rd., Ann Arbor, MI 48103.]

——, and K. Peters, 1981: The smoothing spline: A new approach standardizing forest interior tree-ring series for dendroclimatic studies. *Tree Ring Bull.,* **41,** 45–53.

——, and R. L. Holmes, 1986: User's manual for Program ARSTAN (chronology series VI). University of Arizona, 182 pp.

——, and L. A. Kairiukstis, 1990: *Methods of Dendrochronology: Applications in the Environmental Sciences*. Kluwer Academic, 394 pp.

Donoso, G., J. Cansino, C. Soler, and J. Prieto, 1999: Economic impact of drought in Chilean agriculture. *Drought in Chile: Causes, Consequences and Amelioration* (in Spanish), A. Norero and C. Bonilla, Eds., Pontificia Universidad Católica, 53–70.

Douglass, A. E., 1941: Crossdating in dendrochronology. *J. For.,* **39,** 825–828.

Draper, N. R., and H. Smith, 1981: *Applied Regression Analysis.* 2d ed. John Wiley & Sons, 709 pp.

Fritts, H. C., 2001: *Tree Rings and Climate*. Blackburn Press, 567 pp.

——, and T. W. Swetnam, 1989: Dendroecology: A tool for evaluating variations in past and present forest environments. *Adv. Ecol. Res.,* **19,** 111–188.

Gilliss, J. M., 1855: *The U.S. Naval Astronomical Expedition to the Southern Hemisphere During the Years 1849–'50–'51–'52.* Vol. 1, *Chile; Its Geography, Climate, Earthquakes, Government, Social Condition, Mineral And Agricultural Resources, Commerce,* A. O. P. Nicholson, 556 pp.

Holmes, R. L., 1983: Computer-assisted quality control in tree-ring dating and measurement. *Tree-Ring Bull.,* **44,** 69–78.

Houghton, J. T., Y. Ding, D. J. Griggs, M. Noguer, P. J. van der Linden, X. Dai, K. Maskell, and C. A. Johnson, Eds., 2001: *Climate Change: The Scientific Basis*. Cambridge University Press, 881 pp.

IMSL, 1982: *IMSL Library Reference Manual.* 9th ed. Vol. 2. IMSL, Inc., FTFREQ-1–FTFREQ-5.

INE, 2003: *Population Census 2002* (in Spanish). Vol. 1. Instituto Nacional de Estadísticas, 356 pp.

Jenkins, G. M., and D. G. Watts, 1968: *Spectral Analysis and Its Applications*. Holden-Day, 525 pp.

Jones, P. D., cited 2005: Southern Oscillation Index (SOI). [Available online at http://www.cru.uea.ac.uk/cru/data/pci.htm.]

Kaennel, M., and F. H. Schweingruber, Eds., 1990: *Multilingual Glossary of Dendrochronology*. Swiss Federal Institute for Forest, Snow and Landscape Research, Haupt Publishers, 467 pp.

Kaplan, A., M. A. Cane, Y. Kushnir, A. C. Clement, M. B. Blumenthal, and B. Rajagopalan, 1998: Analyses of global sea surface temperature 1856–1991. *J. Geophys. Res.,* **103,** 18 567–18 589. [Update to 2005 available online at http://www.cdc.noaa.gov/cdc/data.kaplan_sst.]

LaMarche, V. C., R. L. Holmes, P. W. Dunwiddie, and L. G. Drew, 1979: *Chile*. Tree-Ring Chronologies of the Southern Hemisphere Series V, Vol. 2, Laboratory of Tree-Ring Research, University of Arizona, 43 pp.

Le Quesne, C., 1999: Dendrochronology of *Austrocedrus chilensis* (D. Don) Pic. Ser. et Bizz. (*Cupressaceae*), in the northern limit of distribution, Chile (in Spanish). Ph.D. dissertation, Universidad de Oviedo, Asturias, Spain, 89 pp.

Like, J., 1980: Variance of MVUE for lognormal variance. *Technometrics,* **22,** 253–258.

Luckman, B. H., and R. Villalba, 2001: Assessing the synchroneity of glacier fluctuations in the western Cordillera of the Americas during the last millennium. *Interhemispheric Climate Linkages,* V. Markgraf, Ed., Academic Press, 119–140.

Maldonado, G., 1999: Economy: Figures reveal the worst semester in the last 16 years (in Spanish). *El Mercurio,* 24 August, A01.

Masiokas, M. H., R. Villalba, B. H. Luckman, C. LeQuesne, and J. C. Aravena, 2006: Snowpack variations in the central Andes of Argentina and Chile, 1951–2005: Large-scale atmospheric influences and implications for water resources in the region. *J. Climate,* in press.

Miller, A., 1976: The climate of Chile. *Climates of Central and South America,* W. Schwerdtfeger, Ed., Elsevier, 113–145.

Montecinos, A., and P. Aceituno, 2003: Seasonality of the ENSO-related rainfall variability in central Chile and associated circulation anomalies. *J. Climate,* **16,** 281–296.

Ortlieb, L., 1994: Major historical rainfalls in central Chile and the chronology of ENSO events during the XVI-XIX centuries (in Spanish). *Rev. Chil. Hist. Nat.,* **67,** 463–485.

——, 2000: The documentary historical record of El Niño events in Peru: An update of the Quinn record (sixteenth through nineteenth centuries). *El Niño and the Southern Oscillation, Multiscale Variability, Global and Regional Impacts,* H. F. Diaz and V. Markgraf, Eds., Cambridge University Press, 207–295.

Piwonka, G., 1999: *The Waters of Santiago de Chile 1574–1741* (in Spanish). Editorial Universitaria, 480 pp.

Quinn, W. H., and V. T. Neal, 1983: Long-term variations in the Southern Oscillation, El Niño, and the Chilean subtropical rainfall. *Fish. Bull.,* **81,** 363–374.

Quintana, J., 2000: The drought in Chile and La Niña. *Drought Network News,* Vol. 12, No. 2, University of Nebraska at Lincoln, 3–6.

——, 2004: Factors involved in the interdecadal precipitation variability in Chile (in Spanish). M.S. thesis, Department of Geophysics, Universidad de Chile, 88 pp.

Rasmusson, E. M., X. Wang, and C. F. Ropelewski, 1990: The biennial component of ENSO variability. *J. Mar. Syst.,* **1,** 71–96.

Rivas, F., 1999: Yesterday in the Metropolitan region: The traffic was the most affected by the electricity shortages (in Spanish). *El Mercurio*, 7 April, A01.

Rivera, A., G. Casassa, C. Acuña, and H. Lange, 2000: Recent glacier variations in Chile (in Spanish). *Rev. Invest. Geogr.,* **34,** 29–60.

Rutlland, J., and H. Fuenzalida, 1991: Synoptic aspects of the central Chile rainfall variability associated with the Southern Oscillation. *Int. J. Climatol.,* **11,** 63–76.

SAS Institute, Inc., 1999: The GLM procedure. *SAS/STAT User's Guide, Version 8,* SAS Institute, Inc., 1467–1636.

Schulman, E., 1956: *Dendroclimatic Changes in Semiarid America*. University of Arizona Press, 142 pp.

Snee, R. D., 1977: Validation of regression models: Methods and examples. *Technometrics,* **19,** 415–428.

Steel, R. G. D., and J. H. Torrie, 1980: *Principles and Procedures of Statistics.* 2d ed. McGraw-Hill, 633 pp.

Stokes, M. A., and T. L. Smiley, 1996: *An Introduction to Tree-Ring Dating.* 2d ed. University of Arizona Press, 73 pp.

Taulis, E., 1934: De la distribucion de pluies au Chili. *Matér. Étude Calamités,* **33,** 3–20.

Van Husen, Ch., 1967: Climate classification of Chile based upon probability distribution of precipitation totals (in German). Ph.D. thesis, Institute of Geography, Albert-Ludwigs-Universität Freiburg, 113 pp.

Vicuña Mackenna, B., 1970: *The Climate of Chile* (in Spanish). 2d ed. Editorial Francisco de Aguirre, 399 pp.

Viessman, W., T. E. Harbaugh, and J. W. Knapp, 1972: *Introduction to Hydrology*. Intext Educational Publishers, 415 pp.

Villalba, R., 1994a: Tree-ring and glacial evidence for the medieval warm epoch and the Little Ice Age in Southern South America. *Climatic Change,* **26,** 183–197.

——, 1994b: Climatic fluctuations in mid-latitudes of South America during the last 1000 years: Their relationships to the Southern Oscillation (in Spanish). *Rev. Chil. Hist. Nat.,* **67,** 453–461.